

Author's Response to Reviews of

Modeling magnetopause location for 4D drift-resolved radiation belt codes: Salammbô model implementation.

Rabia Kiraz, Nour Dahmen, Vincent Maget, Benoit Lavraud

Response to referee comments from Reviewer 2

We would like to thank the referee for the constructive feedback on this article. We have strived to address all the remarks and comments, for which we report our detailed response below.

This paper developed a magnetopause location model which considered the drifting effects based on statistical analysis of observational data. The produced magnetopause model is dependent on L^ , MLT, and Kp index. The model is an important component to global Fokker-Planck models, providing constrains on the simulation boundaries and magnetopause shadowing. The semi-analytical format of the model also makes it an efficient model. This paper studied an important subject and is recommended to be published after the following minor issues are resolved.*

1. *In Figure 5, the author used a linear fit for the Kp dependence at MLT of 10. The curve shown, however, seems closer to a parabolic fit. Can the author explain why a linear fit is used instead of any higher order fit?*

In our opinion, a parabolic fit that curves upward is unrealistic, as bump appears artificial and the plateau at high Kp is likely due to both physical factors and statistical limitations. This is why a linear fit appeared more physically meaningful for us. Nevertheless, during the model construction we tested a higher-order fit. Figure 4 illustrates the parabolic fit (dashed green line) and the linear regression fit (dashed red line) used for describing the evolution of L^*_{mp} at MLT 10H as a function of Kp . The comparison between the two fits in figure 5, shows that using a higher order fit has no significant impact on the final RMSE of the model. Therefore, for the sake of simplicity, we opted for a linear fit. We do not believe that further discussion on this topic is necessary to be added in the paper.

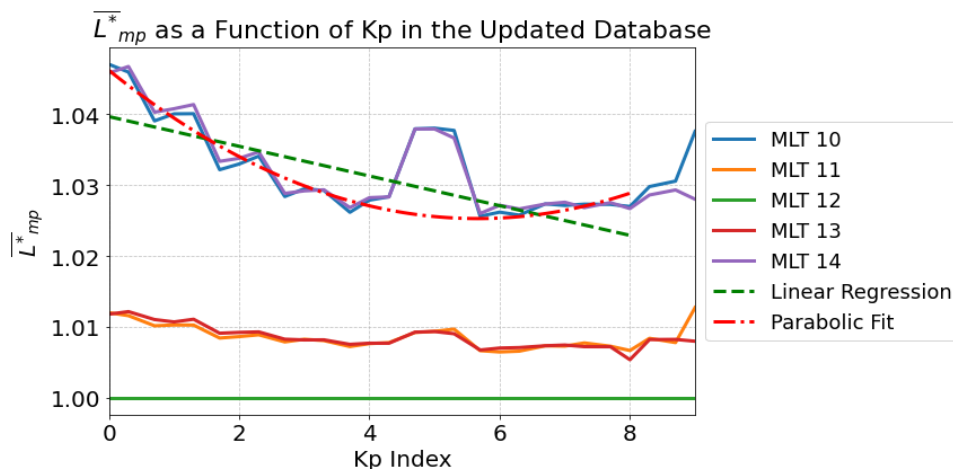


Figure 1: L values of the magnetopause for different MLT values as a function of Kp with a linear regression fit (dashed red line) and a parabolic fit (dashed green line).

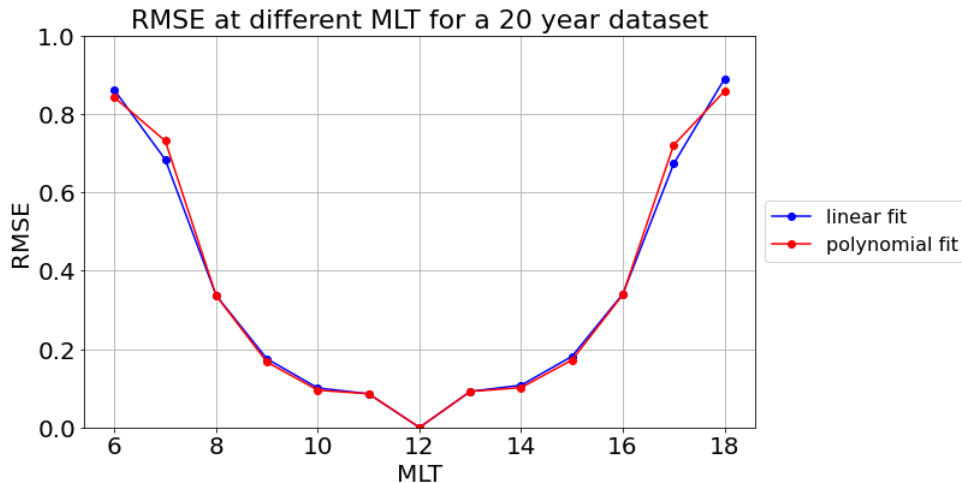


Figure 5: RMSE comparison between a polynomial fit and a linear fit in the model construction.

2. Line 93: “modelmodeling” is a typo.

Line 93 will be amended with the suppression of the typo.

3. Line 318 “The documented dawn-dusk asymmetry of the magnetopause during disturbed times.”: This sentence is incomplete.

Line 318 will be amended with the completion of the sentence.

4. Figure 10: The color-bar makes it hard to distinguish the performances of 3D and 4D models. It is suggested that the author changes a color-bar or chooses a different format for the figure.

Figure 10 will be amended with a new color-bar colormap and a new color-bar unit with relative ratio in percentages.

5. The author provided many discussions on the importance of a MLT dependent magnetopause model in the FP simulations. However, it is not shown or discussed, how the new 4D model will affect the simulations, aside from reducing the boundary error to below the grid sizes. The author should present some discussions, or preferably simulation results with the new 4D model.

Reviewer 1 had the same comment and we acknowledge that this part was missing in our initial paper. To that effect we incorporated an additional section to our paper. This new section focuses on comparing the utilization of 3D versus 4D magnetopause models in Salammbô simulations. To illustrate this comparison, we leveraged a case study of the Saint Patrick geomagnetic storm of March 2015, presenting side-by-side figures of two Salammbô simulation runs: one employing the traditional 3D magnetopause model and the other utilizing our new model. See new section IV below.

IV. Impact of the new magnetopause model in the Salammbô 4D code: The “St. Patrick’s Day” storm in March 2015

The Salammbô 4D code is a modified version of the Salammbô code of Bourdarie et al. (1996) that accounts for the dynamics of low energy electrons. The boundary condition is derived from THEMIS data (Maget et al., 2015) to which a gaussian distribution as a function of MLT centered around midnight has been added to account for this added dimension. The code considers the same

radial diffusion model used in Boscher et al. (2018) and Brunet et al. (2023). The magnetospheric electric field model used to model the convective transport of particles is the UNH-IMEF Matsui et al. (2013) numerical model. Wave particle interactions are taken into account using estimations pitch angle and energy diffusion coefficients from the WAPI code Sicard-Piet et al. (2014) using an MLT dependent classification of VLF waves. Finally, rapid losses from magnetopause shadowing are implemented such that: all particles with an L^* greater than L^* defined by the magnetopause location model are lost.

A comparison between the new and the previous magnetopause models has been made through the simulation of the March 2015 Saint Patrick storm. Results, depicted in Figure 2, showcase the electron phase space density (PSD) on March 17, 2015, at 4:45 am, few times before the storm's peak. Panel (a) depicts the behavior of the 3D model with a MLT-constant L^* value for the magnetopause location equal to L_{mp}^* at MLT 12h. Panel (b) illustrates the behavior of our novel magnetopause model that considers the MLT dependency and allows a more gradual magnetopause shadowing process on the dayside. The ratio between the new model and the previous one can be seen on panel (c), where the PSD ratio globally higher than 1 indicates that more particles are lost with the 3D model than with the 4D one. Although the magnetopause shadowing is only applied to the dayside, ratios are also different from 1 in the nightside. This is due to the electric fields that induce a convective transport of particles (both in MLT and in L^*). Panel (c) highlights the importance of an MLT-dependent magnetopause model, where particles lost in the 3D model are transported to the nightside in the 4D model due to this convective transport mechanism.

Figure 3 supports this assumption by showing the FEDO fluxes at the magnetic equator for 100 keV electrons as a function of MLT on March 17, 2015, at 4:45 AM, based on two Salammbô 4D simulations. The first one uses the 3D magnetopause location model (in blue) while the other one considers the 4D magnetopause location model (in red). Panel (a) illustrates the fluxes of electron at $L^* = 5.4$ where particles get impacted by the magnetopause shadowing and panel (b) shows the fluxes of electron at $L^* = 5$ on a closed drift shell. Both panels illustrate that the 3D model has lower fluxes compared to the 4D one. This means more particles are lost with the 3D model. In contrast, our 4D model preserves these particles, which are transported deeper in the radiation belts. Consequently, we can state that the use of the 3D magnetopause model on a 4D radiation belt code results in excessive loss of low energy particles compared to our new magnetopause model that is MLT dependent.

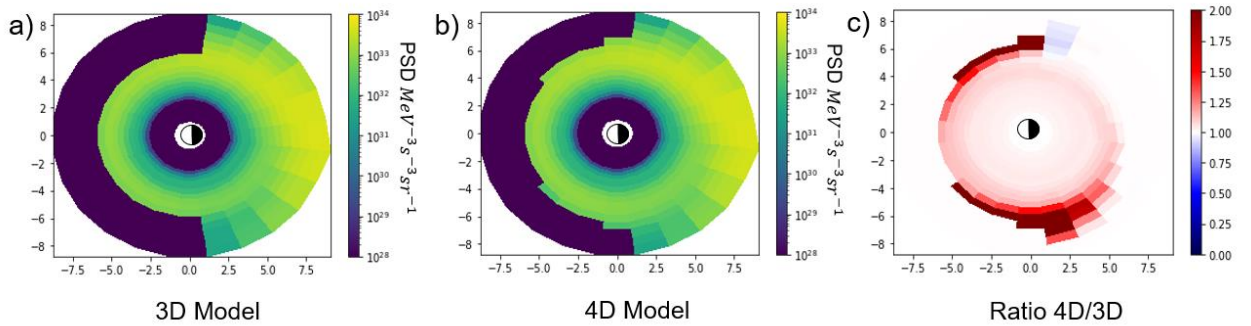


Figure 2: comparison between the phase space density of a Salammbô simulations at $\mu = 5$ MeV/G during the geomagnetic storm of march 2015 with the 3D magnetopause model (panel (a)), the 4D magnetopause mode (panel (b)) and the ratio of the two (panel (c))

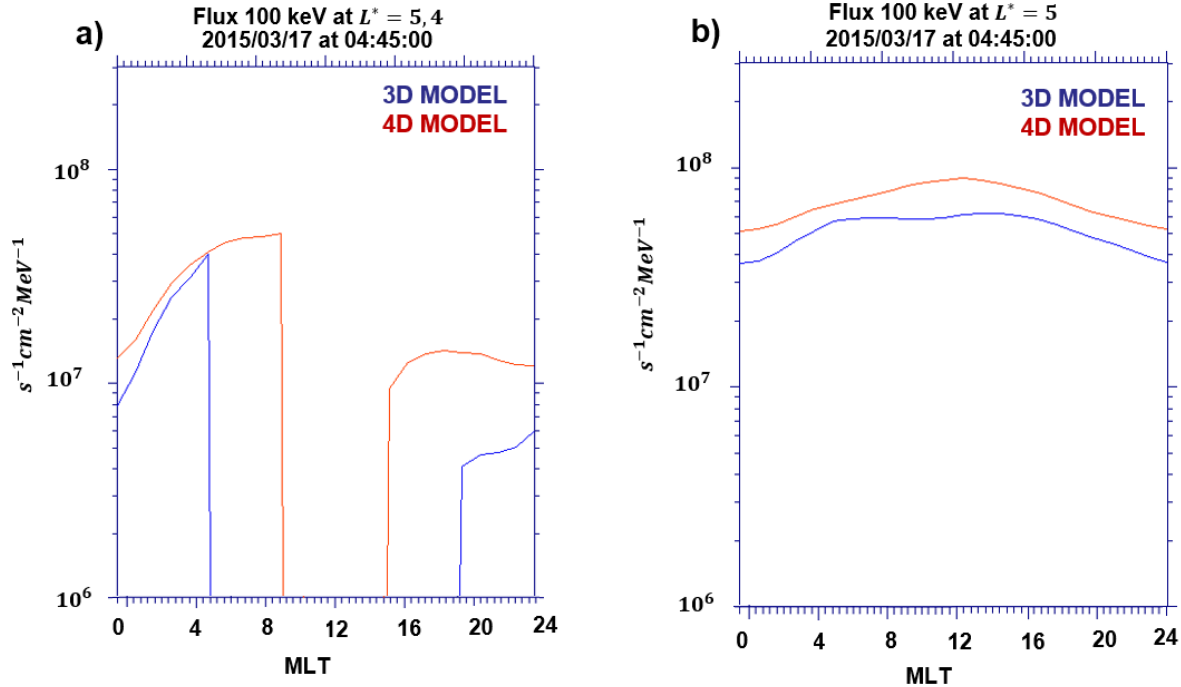


Figure 3: Comparison of FEDO fluxes at the magnetic equator for 100 keV electrons as a function of MLT at a fixed time step during the March 2015 geomagnetic storm, simulated using the Salammbô model. The fluxes are shown for the 3D magnetopause location model (blue) and the new 4D magnetopause location model (red). Panel (a) shows the fluxes at $L^* = 5.4$ and panel (b) at $L^* = 5$.

References

Boscher, D., Bourdarie, S., Maget, V., Sicard-Piet, A., Rolland, G., & Standarovski, D. (2018). High-Energy Electrons in the Inner Zone. *IEEE Transactions on Nuclear Science*, 65(8), 1546-1552. IEEE Transactions on Nuclear Science. <https://doi.org/10.1109/TNS.2018.2824543>

Bourdarie, S., Boscher, D., Beutier, T., Sauvaud, J.-A., & Blanc, M. (1996). Magnetic storm modeling in the Earth's electron belt by the Salammbô code. *Journal of Geophysical Research: Space Physics*, 101(A12), 27171-27176. <https://doi.org/10.1029/96JA02284>

Brunet, A., Dahmen, N., Katsavrias, C., Santolík, O., Bernoux, G., Pierrard, V., Botek, E., Darrouzet, F., Nasi, A., Aminalragia-Giamini, S., Papadimitriou, C., Bourdarie, S., & Daglis, I. A. (2023). Improving the Electron Radiation Belt Nowcast and Forecast Using

the SafeSpace Data Assimilation Modeling Pipeline. *Space Weather*, 21(8), e2022SW003377. <https://doi.org/10.1029/2022SW003377>

Herrera, D., Maget, V. F., & Sicard-Piet, A. (2016). Characterizing magnetopause shadowing effects in the outer electron radiation belt during geomagnetic storms. *Journal of Geophysical Research: Space Physics*, 121(10), 9517-9530. <https://doi.org/10.1002/2016JA022825>

Maget, V., Sicard-Piet, A., Bourdarie, S., Lazaro, D., Turner, D. L., Daglis, I. A., & Sandberg, I. (2015). Improved outer boundary conditions for outer radiation belt data assimilation using THEMIS-SST data and the Salammbo-EnKF code. *Journal of Geophysical Research: Space Physics*, 120(7), 5608-5622. <https://doi.org/10.1002/2015JA021001>

Matsui, H., Torbert, R. B., Spence, H. E., Khotyaintsev, Yu. V., & Lindqvist, P.-A. (2013). Revision of empirical electric field modeling in the inner magnetosphere using Cluster data. *Journal of Geophysical Research: Space Physics*, 118(7), 4119-4134. <https://doi.org/10.1002/jgra.50373>

Nguyen, G., Aunai, N., Michotte de Welle, B., Jeandet, A., Lavraud, B., & Fontaine, D. (2022). Massive Multi-Mission Statistical Study and Analytical Modeling of the Earth's Magnetopause : 2. Shape and Location. *Journal of Geophysical Research: Space Physics*, 127(1), e2021JA029774. <https://doi.org/10.1029/2021JA029774>

Sicard-Piet, A., Boscher, D., Horne, R. B., Meredith, N. P., & Maget, V. (2014). Effect of plasma density on diffusion rates due to wave particle interactions with chorus and plasmaspheric hiss : Extreme event analysis. *Annales Geophysicae*, 32(8), 1059-1071. <https://doi.org/10.5194/angeo-32-1059-2014>

Staples, F. A., Rae, I. J., Forsyth, C., Smith, A. R. A., Murphy, K. R., Raymer, K. M., Plaschke, F., Case, N. A., Rodger, C. J., Wild, J. A., Milan, S. E., & Imber, S. M. (2020). Do Statistical Models Capture the Dynamics of the Magnetopause During Sudden

Magnetospheric Compressions? *Journal of Geophysical Research: Space Physics*, 125(4), e2019JA027289. <https://doi.org/10.1029/2019JA027289>

Xiang, Z., Tu, W., Li, X., Ni, B., Morley, S. K., & Baker, D. N. (2017). Understanding the Mechanisms of Radiation Belt Dropouts Observed by Van Allen Probes. *Journal of Geophysical Research: Space Physics*, 122(10), 9858-9879.
<https://doi.org/10.1002/2017JA024487>